american physiological society | FUNCTION

FUNCTION 7: e106-2025, 2026.
First published March 11, 2026; doi:10.1152/function.106.2025

RESEARCH ARTICLE

Circadian Biology: Timing Matters in Physiology and Pathophysiology

Dietary salt impairs circadian physiological metabolic adaptations in salt-sensitive hypertension

Lashodya V. Dissanayake,[1]* Adrian Zietara,[1]* Ratnakar Tiwari,[1,2] Melissa Lowe,[1] Olha Kravtsova,[1] Vladislav Levchenko,[1] Ruslan Bohovyk,[1] Michelle L. Gumz,[3] and Alexander Staruschenko[1,2,4]

[1]*Department of Molecular Pharmacology & Physiology, Morsani College of Medicine, University of South Florida, Tampa, Florida, United States;* [2]*Hypertension and Kidney Research Center, University of South Florida, Tampa, Florida, United States;* [3]*Department of Physiology and Aging, University of Florida, Gainesville, Florida, United States; and* [4]*James A. Haley Veterans' Hospital, Tampa, Florida, United States*

Abstract

The body's circadian rhythm is coordinated by core clock proteins [period (PER), cryptochrome circadian regulator (CRY), circadian locomotor output cycles kaput (CLOCK), and basic helix-loop-helix ARNT-like protein 1 (BMAL1)] that function in both the central hypothalamic and peripheral tissue molecular clocks. Our recent study demonstrated that deletion of *Per1* in Dahl salt-sensitive (SS) rats ($SS^{Per1-/-}$) exacerbated SS hypertension (HTN), kidney injury, and disrupted blood pressure rhythms. To define time-of-day-, genotype-, and diet-dependent alterations in the renal transcriptome and proteome associated with SS HTN, kidney cortex samples were collected from SS and $SS^{Per1-/-}$ rats fed either a normal-salt (NS, 0.4% NaCl) or high-salt (HS, 4% NaCl) diet, during both the active (night) and inactive (day) periods. Dietary challenges were conducted for 3 wk in male rats. Bulk RNA-sequencing was performed on both NS- and HS-fed groups, and proteomic analyses were performed in HS-fed groups. In SS rats, HS intake blunted time-of-day-dependent transcriptional changes. Pathway analyses predicted significant stress and immune responses, as well as metabolic adaptations, induced by the HS diet. Specifically, the remodeling of the pyruvate dehydrogenase complex was identified as a key prediction in both transcriptomic and phosphoproteomic datasets. As expected, *Per1* deletion further exacerbated disruptions in immune regulation and metabolic adaptation. Collectively, these findings demonstrate that numerous renal genes exhibit diurnal oscillations under physiological conditions and are profoundly disrupted in SS HTN, likely contributing to impaired kidney function and circadian misalignment of blood pressure regulation.

clock genes; Dahl salt-sensitive rat; diurnal variation; kidney transcriptomics; PER1

INTRODUCTION

Salt-sensitive hypertension (SS HTN) is a condition characterized by a significant increase in blood pressure in response to high salt (HS, high NaCl) intake, often associated with renal damage, as the kidneys play a significant role in blood pressure regulation by managing sodium balance and fluid volume. Many mechanisms have been extensively explored in the context of SS HTN, including those related to the sympathetic nervous system, vascular dysfunction, and renal dysfunction (reviewed in Ref. 1). Research over the past few decades has acknowledged that certain inherent factors, like age and sex, also play a role in these conditions (reviewed in Refs. 1–3). One such factor that has gained attention in the context of SS HTN and the kidney is the intrinsic biological mechanism known as the circadian clock (reviewed in Refs. 4–12).

The regulation of the body's circadian rhythm is handled by a central clock located in the hypothalamus and peripheral clocks located in various tissues, such as the kidneys and heart. These clock mechanisms are mainly orchestrated by four core proteins (i.e., clock proteins): basic helix-loop-helix ARNT-like protein 1 (BMAL1), circadian locomotor output cycles kaput (CLOCK), period (PER), and cryptochrome circadian regulator (CRY). Together with additional regulatory clock components, these proteins coordinate the rhythms of blood pressure and renal function, cued by external factors such as light and feeding (reviewed in Ref. 6). Because humans are diurnal (active during the day and sleeping at night), in normotensive subjects, nighttime blood pressure drops by 10%–20% (dippers). However, patients with SS HTN frequently exhibit an attenuated or absent nocturnal blood pressure decline (nondippers), a phenotype

*L. V. Dissanayake and A. Zietara contributed equally to this work.
Correspondence: A. Staruschenko (staruschenko@usf.edu); L. V. Dissanayake (lashodya@usf.edu).
Submitted 24 November 2025 / Revised 20 February 2026 / Accepted 26 February 2026

associated with disruptions in circadian regulation of renal sodium excretion (13–15).

Numerous studies in animal models have demonstrated that loss of even a single clock protein can profoundly alter cardiovascular and renal phenotypes (8, 16–20). To this end, our previous research showed that knocking out *Per1* in Dahl SS rats ($SS^{Per1-/-}$) exacerbated HTN and accelerated kidney injury when rats were fed a HS diet (8). Interestingly, this study further demonstrated that although the animals were housed under a standard 12:12 light:dark cycle, the $SS^{Per1-/-}$ rats exhibited a desynchronized blood pressure rhythm, in which the peak time of blood pressure became highly variable among individual animals, when challenged with HS, but not under a normal-salt (NS) diet. Despite these observations, the mechanisms through which PER1 modulates the SS phenotype remain incompletely understood.

A recent study conducted on Dahl SS rats also showed that time-restricted feeding without salt restriction can be an effective way to prevent further increases in blood pressure and kidney damage in SS rats, highlighting the importance of time-of-day as a key biological variable in this disease (21). Despite clear evidence of circadian rhythm disruption in human SS HTN and the widespread use of Dahl SS rats as an experimental model, little is known about how time-of-day influences renal gene expression patterns in this strain. The few studies that have addressed this topic were conducted more than two decades ago and relied on microarray or qPCR-based approaches (9, 12). To determine how time-of-day, genotype, and diet influence the renal transcriptome and proteome of SS rats and to identify pathways for future mechanistic investigation, we performed a comprehensive multiomics study. Our findings reveal that dietary salt loading, time-of-day, and PER1 deficiency each significantly impact kidney gene expression, predicting to affect pathways linked to HTN, circadian regulation, immune responses, and renal injury. Moreover, the data suggest substantial time-of-day-dependent metabolic reprogramming within the kidneys of salt-challenged animals.

MATERIALS AND METHODS

Animal Models and Experimental Design

All rats were maintained under a 12:12-h light-dark cycle [with the lights off (dark) from 6:00 PM to 6:00 AM) and provided with a standard salt diet [normal salt (NS), 0.4% NaCl, Dyet# 113755, Dyets Inc., Bethlehem, PA], with food and water available ad libitum. All animal procedures adhered to the guidelines specified in the National Institutes of Health Guide for the Care and Use of Laboratory Animals. Each protocol involving rats received review and approval from the University of South Florida Institutional Animal Care and Use Committee (IACUC). Dahl salt-sensitive (SS/JrHsdMcwi, RRID: RGD_61499 and SS-$Per1^{em3Mcwi}$, $SS^{Per1-/-}$, RRID: RGD_13825147) strains were bred in-house. The generation and characterization of $SS^{Per1-/-}$ have been described previously (8, 10).

Male SS and $SS^{Per1-/-}$ rats at 8 wk of age were either challenged with a high-salt (HS, 4% NaCl Dyet# 113756, Dyets Inc., Bethlehem, PA) diet or continued on the NS diet for 3 wk. An essential consideration for rodent models in circadian clock studies is that they are nocturnal (active at night and sleeping during the day), rather than diurnal. Therefore, the daytime will be referred to as the inactive period of the rat, and the nighttime will be referred to as the active period of the rat. The rats were euthanized under anesthesia [2%–3% (vol/vol) isoflurane] either at 2:00 PM (the daytime or inactive period of the rat) or 2:00 AM (the nighttime or active period of the rat). These timepoints were chosen strictly for practical reasons. The time 2:00 PM was selected to match the tissue collected for the previous paper characterizing $SS^{Per1-/-}$ and to align with any published characterization of SS rats; 2:00 AM was selected to provide a 12-h period between the two points. Before euthanasia, the kidneys were perfused with PBS, harvested, and immediately snap-frozen in liquid nitrogen for further analysis. The number of rats collected from the NS-fed SS groups at 2:00 AM and 2:00 PM, and from the NS-fed $SS^{Per1-/-}$ groups at 2:00 AM and 2:00 PM, are 6, 6, 5, and 6, respectively, all of which were used for transcriptomics. The numbers of rats collected from HS-fed SS groups at 2:00 AM and 2:00 PM, and from HS-fed $SS^{Per1-/-}$ groups at 2:00 AM and 2:00 PM, are 5, 5, 6, and 5, respectively. Five samples from each group of HS-fed rats were used for transcriptomics, and 5, 4, 6, and 4 samples were used for proteomics.

RNA Extraction and Sequencing

Total RNA was extracted from the kidney cortices of snap-frozen tissue using Trizol reagent (Thermo Fisher Scientific, Waltham, MA). RNA sequencing (RNA-Seq) was performed commercially by Novogene using the total RNA (UC Davis, CA). In brief, RNA quality was assessed using an Agilent 5400; all samples had RNA integrity number (RIN) $\geq$ 7. mRNA was isolated using magnetic beads, and cDNA was quantified and size-checked using Qubit, PCR, and a Bioanalyzer. Libraries were sequenced on Illumina NovaSeq. Raw data were processed with fastp, mapped with HISAT2, and gene counts ere obtained with featureCounts. Fragments per kilobase of transcript per million mapped reads (FPKM) values were calculated considering gene length and read counts. Differential expressions were analyzed using DESeq2.

Sample Preparation for Proteomics and Phosphoproteomics

All methods relating to mass spectrometry were done at the Morsani College of Medicine Proteomics Core at the University of South Florida. Cells were lysed in radioimmunoprecipitation assay (RIPA) buffer with 1X Halt protease inhibitor cocktail, centrifuged, and transferred to fresh tubes. Samples were prepped using S-TRAP micro spin columns from Protifi LLC (22). In brief, aliquots of 50 µg were treated with 20% SDS to 5% final concentration. Samples were reduced with 20 mM dithiothreitol, heated at 95°C for 10 min, cooled, then alkylated with 40 mM iodoacetamide. Incubated in the dark for 20 min at room temperature, then centrifuged at 17,000 *g* for 10 min to remove undissolved matter. The clarified supernatant was transferred and acidified with 12% phosphoric acid to a final concentration of 1.2%. Six volumes of 90% methanol, 100 mM Tris, pH 7.1, buffer were added to the acidified protein. The mixture was

loaded into an S-Trap microcolumn, centrifuged at 4,000 *g* for 1 min, and the flow-through was discarded; this was repeated until complete. The protein was washed thrice with S-Trap buffer. Proteolytic digestion was performed with 50 mM tetraethylammonium bromide (TEAB) and 1 µg trypsin/Lys-C and incubated overnight at 37°C. Peptides were eluted with TEAB, 0.2% formic acid, and 50% acetonitrile with 0.2% formic acid, then dried and resuspended in 0.1% formic acid in water, sonicated, and centrifuged.

Liquid Chromatography-Mass Spectrometry Analysis

Peptides were characterized using a Thermo Q-exactive-HF-X mass spectrometer coupled to a Thermo Easy nLC 1200. Samples were separated at 300 nL/min using an Acclaim PEPMAP 100 trap (75 µM, 2 cm, c18 3 µm, 100 A) and an Acclaim PEPMAP 100 Column (75 µm, 25 cm, c18, 100 A) using a 120-min gradient with a starting condition of 2% B buffer (0.1% formic acid in 90% acetonitrile) and 98% A buffer (0.1% formic acid in water). Buffer B increased to 28% over 100 min, then to 40% in 10 min, followed by 10 min at 90%. The mass spectrometer used a Thermo nanospray easy source with spray voltage 2.00 kV, capillary temperature 275°C, and funnel radio frequency (RF) level 40. Data acquisition parameters include MS resolution 60,000, AGC target 3e6, max IT 50 ms, range 400–1,600 *m/z*. MS/MS resolution 15,000, AGC 1e4, max IT 50 ms, top 30 peaks, 1.6 m/z isolation window, dynamic exclusion 25 s.

Data Handling for Mass Spectrometry

Samples were processed using MaxQuant 2.0.3.1 software (23). A reviewed rat protein database was downloaded from UniProt and searched with the following parameters: tryptic enzyme with a maximum of 2 missed cleavages, a precursor mass tolerance of 10 ppm, and a fragment mass tolerance of 0.02 Da. Modifications included oxidation; acetylation; phosphorylation of serine (S), threonine (T), and tyrosine (Y) residues (pSTY); and carbamidomethylation. The false discovery rate (FDR) was set at 0.01. Label-free quantification (LFQ) intensities were used for analysis. Data were filtered using Perseus v1.6.12.0 software, requiring groups to have 5 of 6 IDs to be retained in the dataset (24). Ratio and *t* tests were performed on the processed data.

Pathway and Functional Analyses

Pathway analysis was performed using the Qiagen Ingenuity Pathway Analysis (IPA) software (Summer 2025 release) (25). All IPA analyses were performed by a Qiagen IPA-certified analyst.

Filtering for circadian rhythm regulation-related genes was performed as follows: first, the "disease and functions search" tool was used and searched for "circadian rhythm regulation." This revealed 162 genes (the number of genes associated with a term can vary with the software version used, as the knowledge base is continually updated with new literature) that are supported by experimental data and are associated with the term in the IPA knowledge base. Thereafter, we used the "overlay" function in the "my pathway" tool for each comparison to generate the gene lists.

For each comparison, a separate "core analysis" of the expression analysis subtype was conducted through IPA. Any canonical pathways, upstream analyses (upstream regulators, mechanistic networks, and causal networks), diseases, biological functions presented are derived from the results of the core analysis.

We implemented the following steps to select a shortlist of upstream regulators for building graphical summary networks. First, we used the complete list of upstream regulators suggested by IPA for each separate analysis. We then selected only the upstream regulators that are endogenous factors, such as genes, proteins, and microRNAs (excluding exogenous agents, such as chemicals and drugs). We then filtered the list for upstream regulators with predicted activation status (i.e., those with an activation *z*-score $> |2|$). Several of the top upstream regulators by *P* value of overlap were selected for each analysis to construct a network.

"Comparison analysis" between 3 of the core analyses *1*) transcriptomics, NS-fed SS rats active vs. inactive; *2*) HS-fed SS rats active vs. inactive; and *3*) proteomics, HS-fed SS rats active vs. inactive) was conducted. A "comparison analysis" features a heatmap that visualizes upstream regulators across analyses, helping identify trends, clusters, and similarities or differences. Using this feature, we compiled a shortlist of upstream regulators that are common to at least two of the three analyses we considered. Using a *z*-score cutoff of $> |1.5|$, we identified two upstream regulators, whose effects differed in direction between the dietary challenges. Those identified and their downstream effectors were further analyzed through Search Tool for the Retrieval of Interacting Genes/Proteins (STRING) analysis to examine predicted protein interactions and create a network (26).

Phosphoproteomics data were processed using the PhosphoAnalyst platform (Monash Proteomics and Metabolomics Platform & Monash Bioinformatics Platform, Monash University, Australia). Subsequently, Phosphomatics (University of Melbourne, Australia) was used to create the upstream kinase-substrate networks (27). Figures were created using either R, GraphPad Prism, or BioRender. The R packages used to create principal component analysis (PCA) plots were "ggplot2" and "dplyr." Venn diagrams were created using the open-source resource InteractiVenn (28).

Statistical Analysis

GraphPad Prism 10 software was used to perform statistical tests that were not performed by the individual software used for omics analyses. For transcriptomics, an adjusted *P* value less than 0.05 was considered statistically significant. IPA uses a *z*-score algorithm for making predictions (25). This algorithm aims to minimize the likelihood that random data will produce falsely significant predictions. IPA calculates the *P* value of overlap using Fisher's exact test. All details of any additional individual statistical tests for each figure are included in the figure legends.

RESULTS

Salt Loading Blunts the Differential Gene Expression during the Active Period in Dahl SS Rats

In an earlier microarray study, it was shown that gene expression in the livers and kidneys of Dahl SS rats was significantly influenced by time-of-day (9). Furthermore, our

previous research indicated that a global knockout of *Per1* on the Dahl SS background worsened HTN and kidney damage and caused a desynchronization of blood pressure rhythms (8). To examine how time-of-day affects gene expression patterns in the kidneys of SS hypertensive rats and to further explore the effects of PER1 knockout, we performed transcriptomic analyses of kidney cortex tissue from SS and $SS^{Per1-/-}$ rats fed either an NS or HS diet.

NS-fed groups and HS-fed groups were analyzed in separate batches. NS-fed group transcriptomic analysis by PCA showed that the data clustered closely by time-of-day rather than by genotype (Supplemental Fig. S1*A*). By comparison, the PCA for HS-fed groups clustered more closely by genotype than by time-of-day (Supplemental Fig. S1*B*). The number of differentially expressed genes (DEGs; adjusted P value < 0.05) revealed distinct effects of time-of-day, genotype, and diet (Fig. 1, *A* and *B*, and Supplemental Fig. S2, *A* and *B*). In SS rats, the kidney cortex exhibited 2,315 DEGs when comparing the active (night) to the inactive (day) period under an NS diet. However, this rhythmic transcriptional variation was substantially blunted under the HS diet, with only 490 DEGs detected (Fig. 1*A* and Supplemental Fig. S2*A*). In contrast, $SS^{Per1-/-}$ rats displayed a relatively consistent number of DEGs between active and inactive period regardless of dietary intake, with 1,522 DEGs under NS and 1,425 under HS conditions.

Genotypic effect ($SS^{Per1-/-}$ vs. SS) had minimal impact on gene expression during the inactive period under NS conditions, with only 39 DEGs detected (Fig. 1*B* and Supplemental Fig. S2*B*). In contrast, both active period and HS feeding produced substantial transcriptional changes, with higher numbers of DEGs observed across these comparisons (NS at active: 2,984; HS at inactive: 3,038; HS at active: 2,878; Fig. 1*B* and Supplemental Fig. S2*B*). To complement the transcriptomic data, we performed untargeted kidney proteome and posttranslational modification (PTM) profiling (phosphoproteomics) in HS-fed animals. Consistent with transcriptomics, the number of differentially expressed proteins (DEPs) was lower in the time-of-day comparisons than in the genotype comparisons (Fig. 1*C*).

HS Diet Disrupts the Pattern of "Circadian Rhythm Regulation"-Related Gene Expression

To determine whether circadian rhythm-related genes exhibited appropriate changes in expression between the inactive and active periods and genotypes, we filtered the DEG lists for each comparison using the IPA knowledgebase. Among the 162 genes associated with the term "circadian rhythm regulation," 30 were differentially expressed in SS and 17 in $SS^{Per1-/-}$ rats fed an NS diet when comparing the active period with the inactive period (Fig. 2*A*). In contrast, SS rats fed a HS diet displayed fewer circadian-related genes

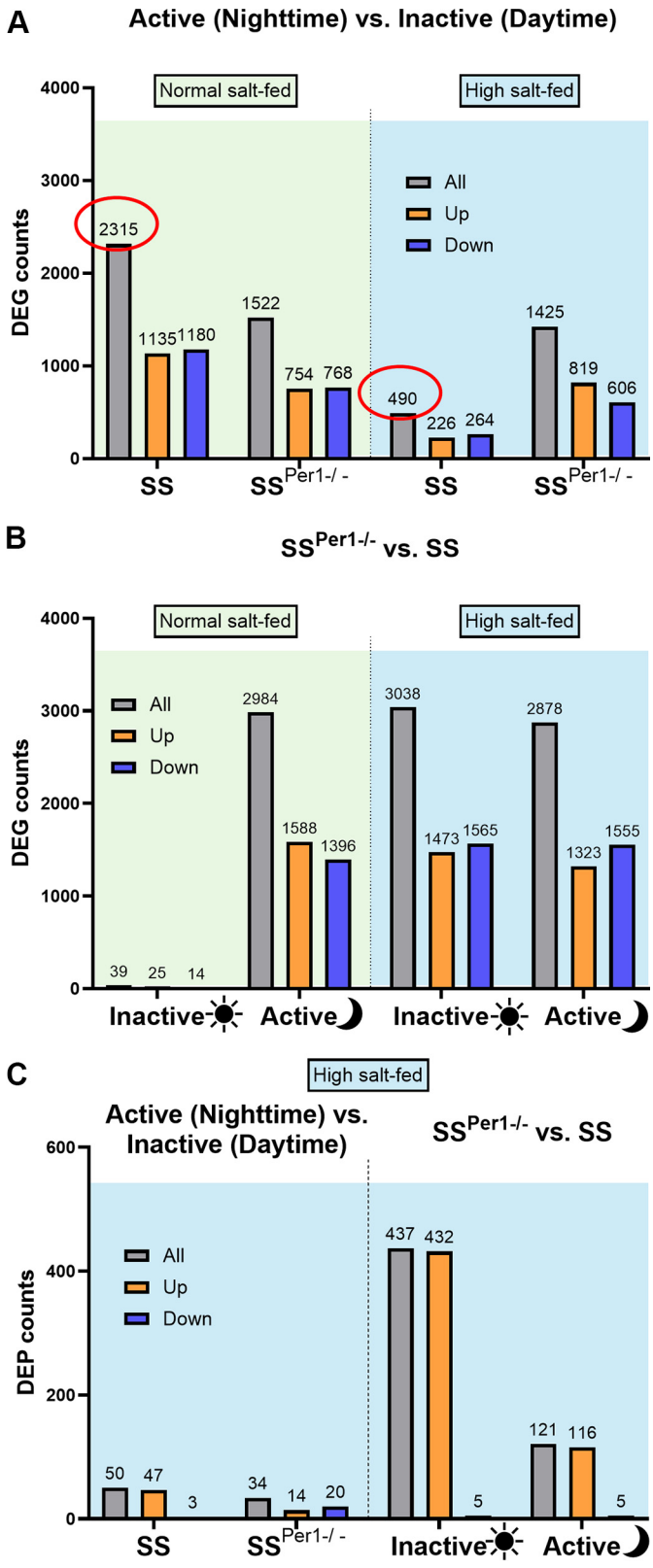

Figure 1. Number of differentially expressed genes (DEGs) and proteins (DEPs) in different transcriptomic/proteomic analyses. *A*: number of DEGs in active vs. inactive period comparisons (i.e., time-of-day effect) in normal-salt-fed and high-salt-fed male Dahl SS and $SS^{Per1-/-}$ rat kidney cortices. *B*: number of DEGs in $SS^{Per1-/-}$ vs. SS comparisons (i.e., genotypic effect) in normal-salt-fed and high-salt-fed male rat kidney cortices collected during the inactive period and active period. Genes that had an adjusted P value < 0.05 and $|\log2FoldChange| \geq 0$ were considered DEGs. *C*: number of DEPs in $SS^{Per1-/-}$ vs. SS comparisons (i.e., genotypic effect) in normal-salt-fed and high-salt-fed male rat kidney cortices collected during the inactive period and active period. Proteins that had a P value $<$ 0.05 and $|\log2FoldChange| \geq 0$ were considered DEPs. $n = 5$ or 6 rats per group. SS, salt sensitive.

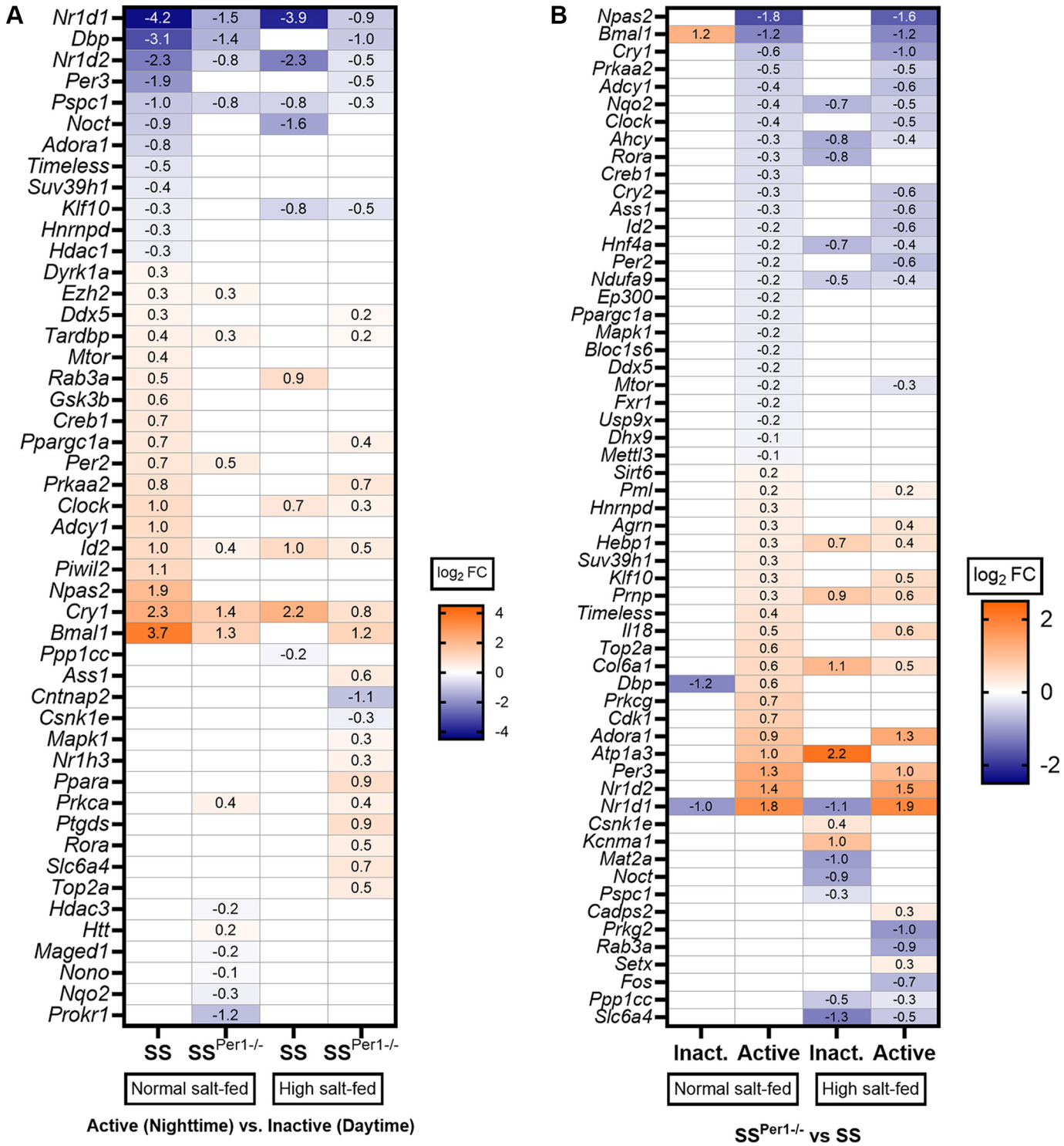

Figure 2. Circadian rhythm regulation-related differentially expressed genes (DEGs) in comparisons within each genotype and dietary challenge. *A*: lists of circadian rhythm regulation-related DEGs affected by the time-of-day (active vs. inactive comparison). *B*: lists of circadian rhythm regulation-related DEGs affected by genotype ($SS^{Per1-/-}$ vs. SS). Filtering for genes was done using the "disease and functions search tool in the" IPA knowledgebase, where 162 genes are associated with the function "circadian rhythm regulation". The "My Pathway" tool's overlay function was used to generate lists of DEGs associated with the term. Genes that had an adjusted *P* value <0.05 were considered DEGs. $n = 5$ or 6 rats per group. IPA, Ingenuity Pathway Analysis; SS, salt sensitive.

that were differentially expressed. $SS^{Per1-/-}$ rats fed a HS diet showed a unique set of circadian-associated DEGs, such as downregulation of contactin-associated protein-like 2 (*Cntnap2*) and casein kinase I isoform epsilon (*Csnk1e*), and upregulation of argininosuccinate synthetase (*Ass1*), mitogen-activated protein kinase 1 (*Mapk1*), nuclear receptor subfamily 1 group H member 3 (*Nr1h3*), peroxisome proliferator-activated receptor alpha (*Ppara*), prostaglandin D2 synthase (*Ptgds*), RAR related orphan receptor A (*Rora*), solute carrier family 6 member 4 (*Slc6a4*), and DNA topoisomerase II alpha (*Top2a*) (Fig. 2*A*).

Disruption of Diurnal Variation by Salt Loading Is Predicted to Affect Stress Response, Immune Response, and Metabolic Adaptations

For further analysis, we used a cutoff of adjusted *P* value $<$ 0.05 and $|\log2FoldChange| \geq 1$, which reduced the number of analysis-ready DEGs. The number of analysis-ready genes is noted in Supplemental Fig. S3.

To examine the master regulators for baseline (SS rats fed an NS diet) and pathological conditions in the time-of-day comparisons, we created summary networks using analysis-ready target molecules and their suggested upstream regulators in IPA (Fig. 3, *A* and *B*). We filtered the full list of significant (*P* value of overlap $<$ 0.05) upstream regulators predicted by IPA for each individual analysis (Supplemental Tables S1 and S2) to shortlist the top endogenous regulators (Supplemental Table S3). When considering only endogenous factors, NS-fed SS rats exhibited 19 upstream regulators with activation/inhibition predictions ($|z$ score$| \geq 2$) at the active period, compared with the inactive period (Supplemental Table S3). Based on the number of shared target molecules, three regulators were selected to build a network [histone deacetylase 1 (HDAC1), interferon-γ (IFNG), and CLOCK] (Fig. 3*A*). HS-fed SS rats showed only four endogenous significant upstream regulators with activation status, all of which were included in the summary network (Fig. 3*B*).

HDAC1 (activation *z* score 2.2), which is known to play a crucial role in epigenetic regulation by removing acetyl groups from histones, leading to chromatin condensation and transcription repression, was suggested to be a driver of the gene expression pattern seen in active compared to the inactive period in SS rats (Fig. 3*A*). This was proposed based on the upregulation of serum/glucocorticoid-regulated kinase 1 (*Sgk1*), SRY-box transcription factor 2 (*Sox2*), peroxisome proliferator activated receptor delta (*Ppard*), tumor protein p73 (*Tp73*), glucocorticoid-induced leucine zipper (*Tsc22d3*), and chromodomain helicase DNA binding protein 9 (*Chd9*) and the downregulation of activating transcription factor 3 (*Atf3*), capping actin protein gelsolin like (*Capg*), lipocalin 2 (*Lcn2*), metallothionein 1 (*Mt1*), metallothionein 2a (*Mt2a*), serpin family E member 1 (*Serpine1*), and secreted phosphoprotein 1 (*Spp1*) genes. Both *Sgk1* and *Tsc22d3* are known to be involved in cellular stress response (29, 30).

Both IFNG (interferon-γ, activation *z* score -2.8) and CLOCK (activation *z* score -2) were suggested to be inhibited upstream regulators affecting many downstream genes. Although some common genes were predicted to be affected by both IFNG and HDAC1, unique gene expressions, such as the upregulation of pyruvate dehydrogenase kinase 4 (*Pdk4*), solute carrier family 4 member 4 (*Slc4a4*), and histone cell cycle regulator (*Hira*) and the downregulation of C-X-C motif chemokine ligand 10 (*Cxcl10*), ChaC glutathione-specific gamma-glutamylcyclotransferase 1 (*Chac1*), and tribbles pseudokinase 3 (*Trib3*), were influenced by IFNG alone. Genes like nuclear receptor subfamily 1 group D member 1 (*Nr1d1*), D-box binding PAR bZIP transcription factor (*Dbp*), and fatty acid synthase (*Fasn*) are predicted to be influenced by both IFNG and CLOCK.

When fed an HS diet, the summary network shifted to indicate tumor necrosis factor (TNF, activation *z* score -2.1), interferon regulatory factor 2 binding protein 2 (IRF2BP2, activation *z* score -2), nuclear receptor subfamily 3 group C member 1 (NR3C1, activation *z* score -2.6), and interleukin 6 (IL6, activation *z* score -2.4) as upstream regulators (Fig. 3*B*). NR3C1, also known as the glucocorticoid receptor (GR), is a central regulator of the metabolic stress response pathway (reviewed in Ref. 31). TNF, IRF2BP2, and IL6 all suggest a shift in immune response based on the differential expression of angiopoietin-like 4 (*Angptl4*), ATPase $H+/K+$ transporting non-gastric alpha2 subunit (*Atp12a*), B-cell lymphoma 6 transcriptonal repressor (*Bcl6*), bone morphogenetic protein 3 (*Bmp3*), cell migration inducing hyaluronidase 1 (*Cemip*), claudin 4 (*Cldn4*), *Fasn*, FosB proto-oncogene AP-1 transcription factor subunit (*Fosb*), gremlin 1 (*Grem1*), inhibitor of DNA binding 3 (*Id3*), insulin-like growth factor binding protein 1 (*Igfbp1*), Kruppel-like factor 5 (*Klf5*), lipopolysaccharide binding protein (*Lbp*), nocturnin (*Noct*), retinoic acid receptor responder 1 (*Rarres1*), and sterol regulatory element binding transcription factor 1 (*Srebf1*). Interestingly, the four regulators in this network are interconnected and can inhibit one another.

HS Feeding Changes the Direction of the Upstream Regulators of Time-of-Day, GR (*Nr3c1*), and Prolactin (*Prl*)

Subsequently, we aimed to identify candidate upstream regulators shared between the NS- and HS-fed groups but that function in opposite directions within each dietary challenge. A comparison analysis of 3 different analyses: *1*) transcriptomics of active versus inactive SS rats fed an NS diet; *2*) transcriptomics of active versus inactive SS rats fed an HS diet; and *3*) proteomics of active versus inactive SS rats fed an HS diet was performed. The top 20 upstream regulators from this analysis were identified (Fig. 4*A*). Only two were directionally different between the NS and HS comparisons (*z*-score cutoff of $> |1.5|$): PRL and NR3C1. PRL (encoding prolactin) was predicted to be inhibited in NS-fed rats and activated in HS-fed rats during the active period in transcriptomic analysis; this prediction was confirmed by proteomic analysis. NR3C1 was predicted to be activated in NS-fed rats and inhibited in HS-fed rats during the active period. DE genes/proteins that affect the predictions for NR3C1 and PRL are depicted in Fig. 4, *B* and *C*.

To determine whether PRL and NR3C1, as well as the DE genes/proteins, have biological interactions, they were submitted to STRING, a database known for predicting protein-protein interactions (26). The network produced showed significantly more interactions than would be expected for a random set of genes (PPI enrichment *P* value 3.69×10^{-12}) (Fig. 4*D*). One of the top significant biological processes suggested by the analysis was "response to lipid" (FDR 4.22×10^{-8}).

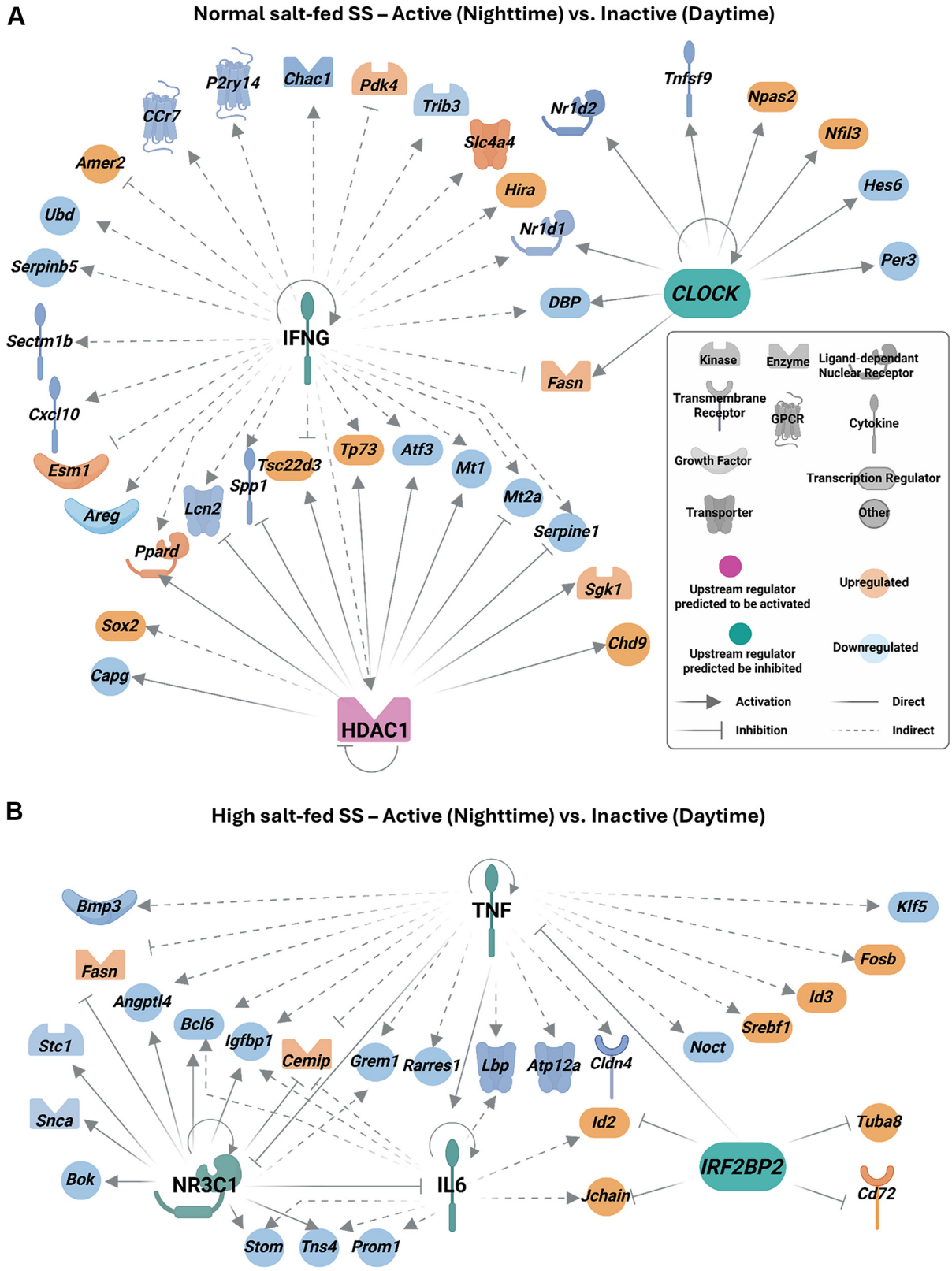

Figure 3. Networks of upstream regulators and downstream differentially expressed genes (DEGs) for the active vs. inactive period comparisons in kidney cortices of male Dahl SS rats fed a normal-salt (*A*) or high-salt (*B*) diet. Upstream regulators are IPA-predicted upstream molecules that may be causing the observed gene expression changes. A few upstream regulators, based on their activation *z*-scores and relationships to one another, are chosen to create these networks. $n = 5$ or 6 rats per group. IPA uses the *P* value of overlap, calculated using the right-tailed Fisher's exact test. IPA, Ingenuity Pathway Analysis; SS, salt sensitive.

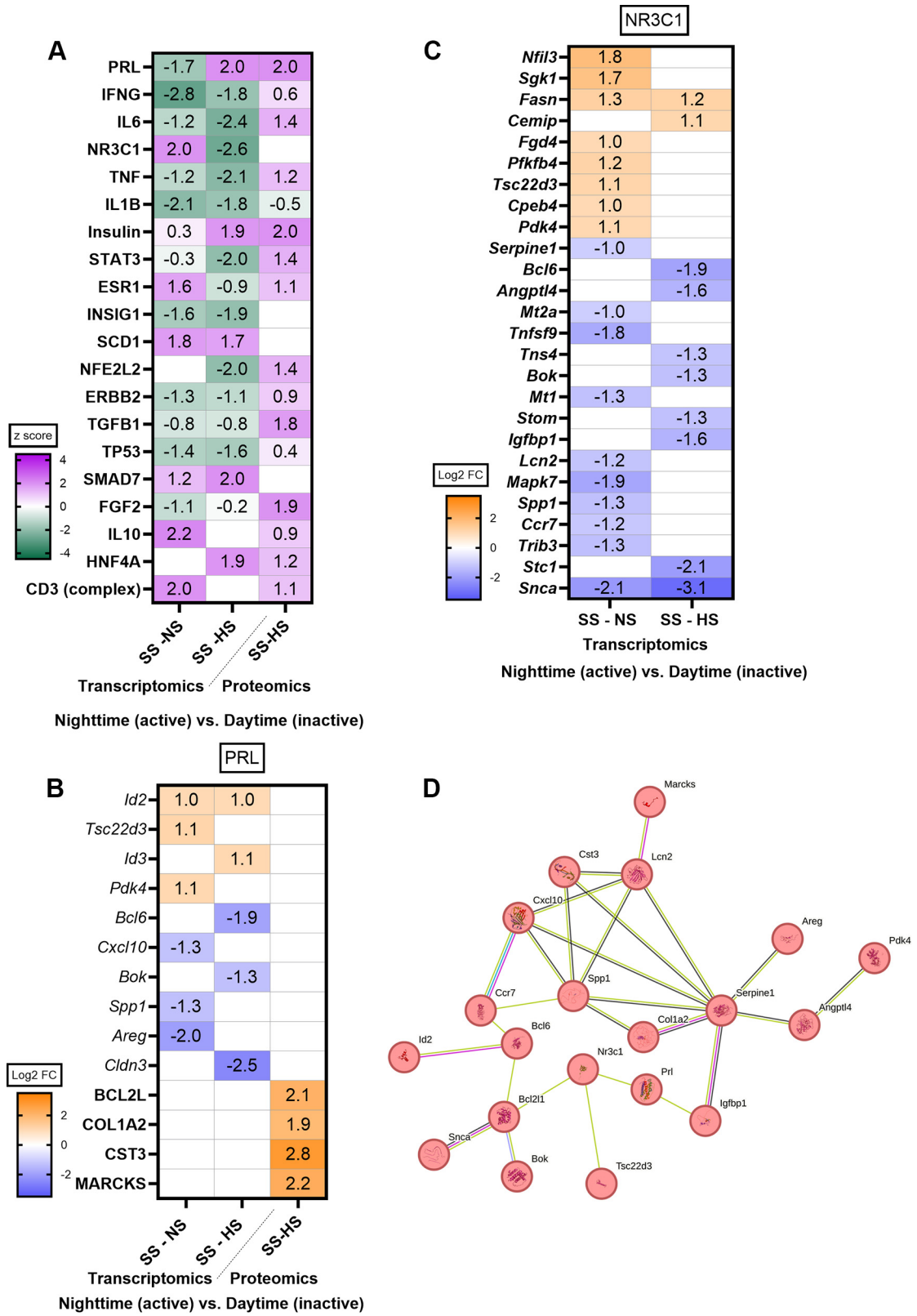

Figure 4. Comparison of top upstream regulators in active vs. inactive period comparisons in transcriptomics and proteomics in different dietary challenges. *A*: top upstream regulators predicted in the comparison analysis of Dahl SS rats, comparing normal-salt (NS) and high-salt (HS) transcriptomics and HS proteomics active vs. inactive periods. Downstream genes or proteins that are differentially expressed suggest PRL (*B*) or NR3C1 (*C*) as an upstream regulator. *D*: STRING network connecting the PRL and NR3C1-related downstream molecules. *z*-Scores ≥ 2 or ≤ -2 are considered significant for predictions. An adjusted *P* value < 0.05 is considered significant. $n = 5$ or 6 per group. SS, salt sensitive.

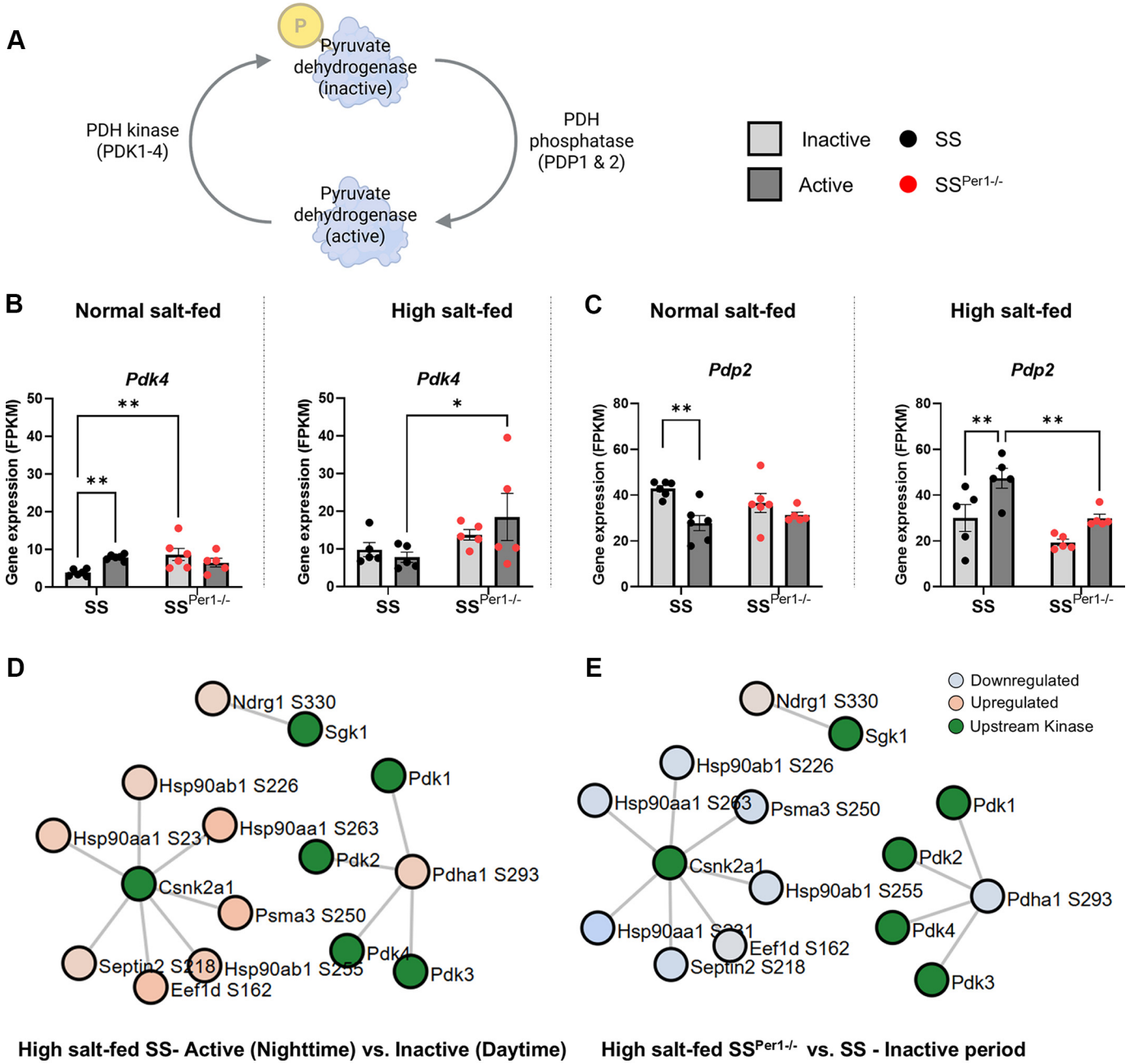

Figure 5. Gene expression of the pyruvate dehydrogenase (PDH) complex enzymes. *A*: schematic of PDH complex. *B*: gene expression of *Pdk4*. *C*: *Pdp2* in SS and SS$^{Per1-/-}$ rat kidney cortices during inactive and active periods when fed a normal-salt or high-salt diet. **P* value < 0.05; ***P* value $<$ 0.01. Network of kinase-substrate connections based on the phosphoproteomic analysis of high-salt-fed SS active vs. inactive comparison (*D*) and high-salt-fed SS$^{Per1-/-}$ vs. SS comparison in inactive period (*E*). $n = 5$ or 6 per group for transcriptomics and 4–6 per proteomics. Two-way ANOVA with multiple comparisons was used for statistical analysis of *B* and *C*. SS, salt sensitive.

The Circadian Control of the Pyruvate Dehydrogenase Complex (PDC) Remodels in Response to HS Intake and the Lack of PER1

The identification of the PRL-NR3C1 network as a key player led us to investigate whether the response to lipid is shifting with time-of-day, genotype, and dietary stress. The checkpoint for switching from glucose to lipid as an energy source in the body is the PDC (Fig. 5*A*). The enzymes pyruvate dehydrogenase kinases (PDK1-4) deactivate this complex through phosphorylation, whereas pyruvate dehydrogenase phosphatases (PDP1 and 2) activate it (reviewed in Ref. 32). Activation of PDC leads to the conversion of pyruvate into acetyl-CoA and the entry of glycolytic products into the tricarboxylic acid (TCA) cycle. In contrast, inactivation of the complex leads to decreased glucose use.

In the current study, NS-fed SS rats showed an increase in *Pdk4* mRNA levels from inactive to active period, whereas SS$^{Per1-/-}$ rats showed no such time-of-day variation (Fig. 5*B*). Upon switching to an HS diet, this active period increase in *Pdk4* expression was not present in SS rats. Interestingly, *Pdp2* was downregulated in NS-fed SS rats during the active

period compared with inactive, whereas switching to HS significantly elevated its expression (Fig. 5*C*). Once again, these diurnal expression patterns were absent in $SS^{Per1-/-}$ rats.

Next, to determine whether the observed changes in kinase expression were reflected at the posttranslational level, we analyzed phosphorylation patterns using phosphoproteomic data from the HS-fed groups. The identified PTMs were analyzed through an open-source platform Phosphomatics (33). A total of 69 phosphorylation sites across 55 unique proteins were identified as suitable for the analysis. Network summary of kinase-substrate interactions revealed that the serine 293 site of pyruvate dehydrogenase (PDH, encoded by *Pdha1*) is phosphorylated at a higher fold in SS rats at active versus inactive period (Fig. 5*D*). Conversely, in $SS^{Per1-/-}$ rats compared with SS rats in the daytime, phosphorylation of PDH at serine 293 was at a lower fold (Fig. 5*E*). In addition, the analysis indicated that *N*-myc downstream regulated 1 (NDRG1) phosphorylation, which is suggested to be affected by SGK1, and multiple PTMs, predicted to be influenced by casein kinase 2 (encoded by *Csnk2a1*) (Fig. 5, *D* and *E*).

Canonical Pathways of the Circadian Clock and Lipid Metabolism Are Predicted to be Activated in NS-Fed but Not HS-Fed Rats in a Time-of-Day-Dependent Manner in SS Rats

The core analyses provided predicted canonical pathways for each analysis. Predictions from IPA provide an intersection between well-characterized metabolic, reactome, and signaling pathways and the data we provide. Supplemental Tables S4–S7 show the full list of statistically significant [$-\log(P \text{ value}) > 1.3$] canonical pathways for SS NS-fed active versus inactive, SS HS-fed active versus inactive, $SS^{Per1-/-}$ NS-fed active versus inactive, and $SS^{Per1-/-}$

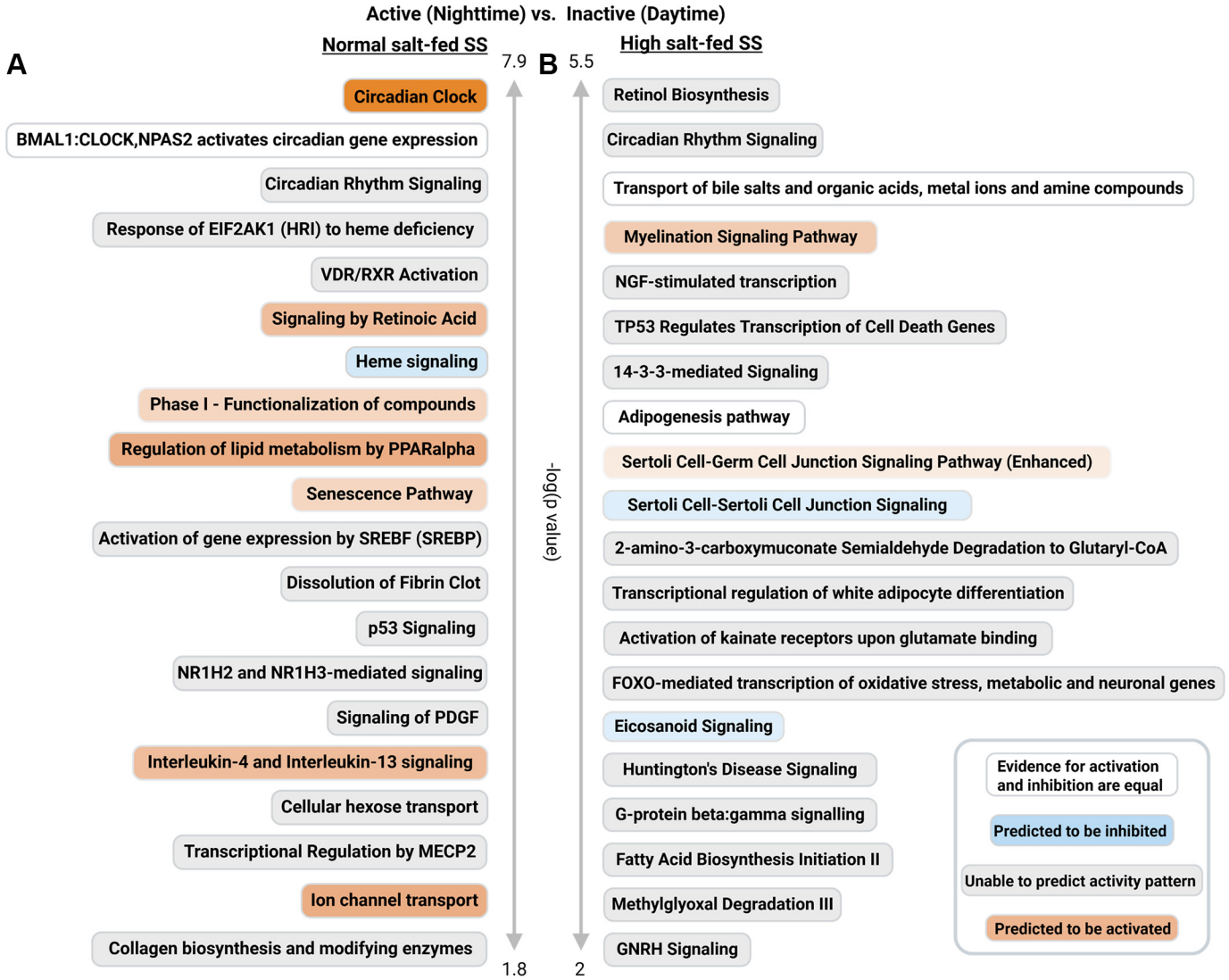

Figure 6. Top 20 canonical pathways enhanced in male Dahl SS rat kidneys during the active compared to inactive period under different diets. Top 20 enhanced canonical pathways arranged by *P* value in normal-salt-fed (*A*) and high-salt-fed (*B*) rat kidney cortex transcriptome. A $-\log(P \text{ value}) > 1.3$ was considered significant. $n = 5$ or 6 rats per group. IPA uses the *P* value of overlap, calculated using the right-tailed Fisher's exact test, to identify significant pathways. The overall activation/inhibition states of canonical pathways are predicted based on a *z*-score algorithm. The pathway coloring was based on the activation status provided by IPA. IPA, Ingenuity Pathway Analysis; SS, salt sensitive.

HS-fed active versus inactive comparisons, respectively. We then identified the top 20 canonical pathways for each analysis based on *P* value and displayed them side by side, grouped by diet, to clearly compare their responses to the dietary challenges (Fig. 6 and Supplemental Fig. S4).

Moving from their inactive period to the active period, the Dahl SS rats on an NS diet had 7/20 pathways with a positive *z*-score (activation): "circadian clock," "signaling by retinoic acid," "phase I—functionalization of compounds," "regulation of lipid metabolism by PPARα," "senescence pathway," and "interleukin-4 and interleukin-13 signaling and ion channel transport" (*z*-score 1.4, 1, 0.4, 1.3, 0.4, 1, 1.3, respectively). Heme signaling was predicted to be inhibited with a *z*-score of −2, whereas all other top pathways were enhanced without a specific direction prediction. On the other hand, the HS challenge shifted most of the top pathways to lack a specific predictive direction. *z*-Scores, in general, had lower confidence. Two of the 20 pathways showed positive (activation) or negative (inhibition) predictions: myelination signaling pathway (*z*-score 1.9), sertoli cell-germ cell junction signaling pathway (*z*-score 0.4), sertoli cell-sertoli cell junction signaling (*z*-score −0.4), and eicosanoid signaling (*z*-score −0.4). Several pathways among the top 20 for the HS-fed time-of-day effect (circadian rhythm signaling, adipogenesis pathway, transcriptional regulation of white adipocyte differentiation, and fatty acid biosynthesis initiation II) were related to the circadian clock and lipid metabolism, but they lacked directional predictions.

Unlike the SS rats, the top 20 predicted pathways for time-of-day comparison in $SS^{Per1-/-}$ rats lacked directionality (Supplemental Fig. S4*A*). Nevertheless, many of the same pathways as SS analysis were predicted, including "circadian clock," "circadian rhythm signaling," "BMAL1: CLOCK, NPAS2 activates circadian gene expression," "signaling by retinoic acid," "heme signaling," "ion channel transport," and "phase I—functionalization of compounds." Interestingly, $SS^{Per1-/-}$ rats fed an HS diet, compared by time of day, did not have any circadian-related pathways in the top 20 (Supplemental Fig. S4*B*).

Gene and Protein Expression in the Absence of *Per1* Is Associated with Predicted Disturbances in Metabolic, Immune, and Circadian Rhythm Adaptations

Our previous study showed that the $SS^{Per1-/-}$ genotype worsened HTN and kidney damage, causing a desynchronization of blood pressure rhythms when fed a HS diet but not a NS diet (8). Although that study confirmed that *Per1* influences the development of SS HTN, it remains unclear which pathways or regulators are involved. Therefore, here we further examine the genotypic effect to identify potential mechanisms.

The top upstream regulators (*z*-score cutoff of $> |1.5|$) for the NS-fed $SS^{Per1-/-}$ versus SS comparison in the inactive period, based on the *P* value of overlap, were corticosterone, NAD-dependent deacetylase sirtuin-1 (SIRT1), growth hormone (family), forkhead box protein O1 (FOXO1), and dexamethasone. The top two were highlighted in Fig. 7*A*. SIRT1 is an enzyme crucial for energy metabolism, playing roles in both lipid and glucose metabolism (reviewed in Ref. 34).

In HS-fed $SS^{Per1-/-}$ rats during the inactive period, there were 1,993 upstream regulators that met the *z*-score cutoff of $>|1.5|$ and *P* value of overlap < 0.05. Some of the top upstream regulators included AGT (encoding for angiotensinogen), aldosterone, and interleukin-1 β (IL1B) (Fig. 7*B*). Among the DEGs that affected the predictions were upregulated oxidized low density lipoprotein receptor 1 (*Olr1*), endothelin 1 (*Edn1*), actin alpha 1 (*Acta1*), brain-derived neurotrophic factor (*Bdnf*), lysyl oxidase (*Lox*), *Serpine1*, heme oxygenase 1 (*Hmox1*), advanced glycosylation end product-specific receptor (*Ager*), LIF-interleukin 6 family cytokine (*Lif*), TIMP-metallopeptidase inhibitor 1 (*Timp1*), periostin (*Postn*), calcium voltage-gated channel auxiliary subunit alpha2delta 1 (*Cacna2d1*), calcium voltage-gated channel subunit alpha1 C (*Cacna1c*), ADAM metallopeptidase with thrombospondin type 1 motif 2 (*Adamts2*), TNF receptor superfamily member 12A (*Tnfrsf12a*), tenascin C (*Tnc*), ADAM metallopeptidase with thrombospondin type 1 motif 1 (*Adamts1*), MYC proto-oncogene (*Myc*), interleukin 1 receptor-like 1 (*Il1rl1*), vimentin (*Vim*), inhibin subunit beta A (*Inhba*), NFKB inhibitor zeta (*Nfkbiz*), transglutaminase 1 (*Tgm1*), inhibitor of nuclear factor kappa B kinase subunit epsilon (*Ikbke*), and pentraxin 3 (*Ptx3*), and downregulated forkhead box P2 (*Foxp2*), angiotensin converting enzyme 2 (*Ace2*), growth hormone receptor (*Ghr*), estrogen receptor 1 (*Esr1*), and iodothyronine deiodinase 1 (*Dio1*). The increase in ET-1 (encoded by *Edn1*) was confirmed in $SS^{Per1-/-}$ in our previous study (10). Increasing the confidence in the predictions, AGT, aldosterone, and IL1B were also identified as upstream regulators in the proteomic analysis (Supplemental Table S8 depicts all common upstream regulators between proteomics and transcriptomics, with an activation $|z\text{-score}| \geq 1.5$).

The top upstream regulators predicted by proteomics for the HS-fed $SS^{Per1-/-}$ versus SS comparison during the inactive period were identified as lipopolysaccharide, PRL, and MLX interacting protein-like (MLXIPL), with activation *z*-scores of 7.1, 4.6, and 4.4, respectively (Supplemental Table S8). *The Mlxipl* gene encodes the carbohydrate-responsive element-binding protein (*ChREBP*), a master regulator of lipogenesis and glucose sensing (reviewed in Ref. 35).

Moreover, both transcriptomics and proteomics from HS-fed $SS^{Per1-/-}$ versus SS comparison predicted 14 overlapping Tox lists in IPA, which included NRF2-mediated oxidative stress response, increased renal damage, renal necrosis, and increased glomerular injury (Supplemental Fig. S5*A*). These predictions align with the previously published characterization of HS-fed $SS^{Per1-/-}$ rats that demonstrated increased fibrosis and medullary protein casts in their kidneys (8).

The canonical pathway analysis of these rats lacking *Per1* when fed a HS diet predicted activation of pathways such as LPS/IL-1-mediated inhibition of RXR function, cardiac hypertrophy signaling, Myc-mediated apoptosis signaling, cardiac β-adrenergic signaling, and endothelin-1 signaling (Fig. 7*C*). Y-glutamyl cycle and aryl hydrocarbon receptor signaling were predicted to be inhibited, whereas the complement system and TWEAK signaling were enhanced with equal evidence for activation and inhibition. Glutathione biosynthesis, CCR5 signaling in macrophages, GABA receptor signaling, and circadian rhythm signaling were enhanced without any directional predictions. Most of these pathways overlapped between transcriptomic and proteomic analyses (Supplemental Fig. S5*B*).

DISCUSSION

Here, we showed that salt loading in SS rats blunts the overall number of DEGs and the diurnal pattern of circadian rhythm-related DEGs when comparing the active with the inactive period. These disruptions were predicted to influence key physiological processes, including stress response, immune response, and metabolic adaptations. Namely, PDC

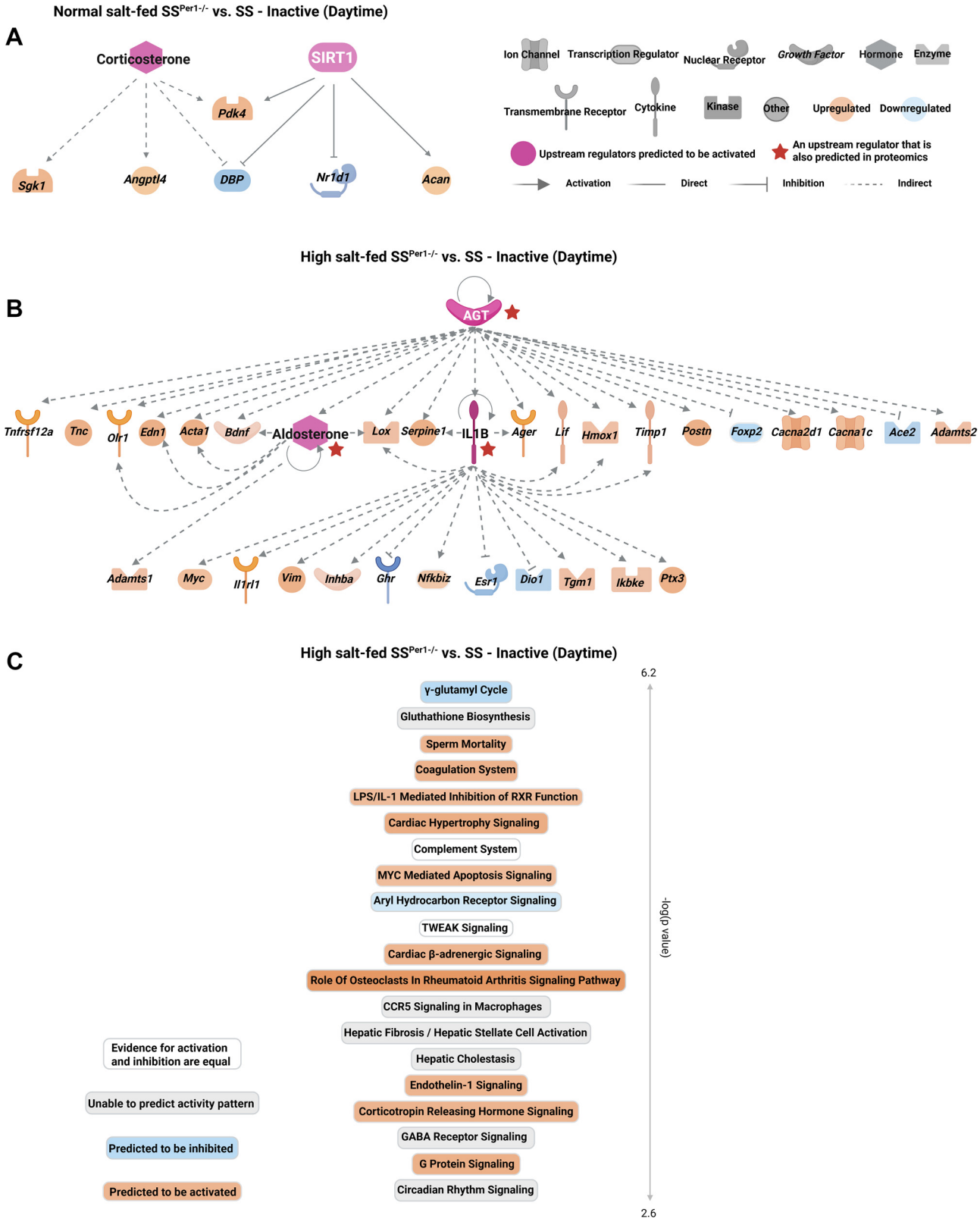

remodeling emerged as a major prediction influenced by upstream regulators, including glucocorticoid receptor (*Nr3c1*) and PRL. The absence of *Per1* was further predicted to exacerbate disturbances in immune regulation and metabolic remodeling, reinforcing its critical role in maintaining normal circadian and metabolic homeostasis.

Clinical findings and our previous research have shown that the salt sensitivity of blood pressure and circadian rhythm are closely intertwined (8). Kimura et al. (4) have further proposed that the interaction between circadian regulation and salt sensitivity is central to understanding the link between cardiovascular and renal comorbidities. In the present study, we aimed to address critical gaps in this area by performing a comprehensive transcriptomic and proteomic analysis of Dahl SS and $SS^{Per1-/-}$ kidney cortices, collected with or without a HS challenge, in both active and inactive periods.

Dahl SS rats have been shown to have significantly elevated blood pressure when fed an HS diet, but not necessarily a desynchrony of the rhythm (8, 12). Furthermore, countless studies have established the persistent kidney damage associated with the SS HTN phenotype (reviewed in Ref. 36). However, whether the whole cortical transcriptome is deregulated in response to salt loading remains unclear. The current study established, for the first time, that time-of-day had a more pronounced effect on gene expression in SS rats when they were relatively healthy (fed an NS diet) than when they were hypertensive (fed an HS diet). Given the significant effects on circadian rhythm signaling identified by IPA analysis, this effect may be a result of changes in the pattern of circadian clock gene expression in response to salt loading. The increased cortical damage observed in hypertensive SS rats may indicate that the number of cortical transcripts is generally lower under salt loading (37).

Interestingly, when *Per1* was knocked out, the time-of-day-dependent pattern of gene expression was absent. This could be associated with the desynchrony of blood pressure rhythm we previously observed in the $SS^{Per1-/-}$ rats (8). These rats, even when fed an NS diet, had a relatively lower number of circadian rhythm-related gene expressions. *Dbp*, a transcriptional activator capable of directly affecting *Per1* expression (38), was downregulated, and *Npas2*, a paralogous gene to *Clock*, was upregulated during the active period (compared to the inactive period) in SS rats. However, these changes were not detected in $SS^{Per1-/-}$ rats, which may contribute to the lack of diet-induced gene expression dampening in the knockouts.

Compared with transcriptomic analyses, proteomic analyses identified fewer differentially expressed proteins (DEPs) overall. In particular, the number of downregulated proteins was extremely low across all analyses. This is likely a methodological limitation. Proteomics based on mass spectrometry (bottom-up LC-MS/MS) is sensitive to protein abundance (unlike transcriptomics), which can be biased toward high-abundance proteins (i.e., upregulation). Nevertheless, several biological factors could also contribute to this effect (posttranscriptional regulation, differential half-lives, and degradation rate, etc.).

Further analyzing DEGs and proteins from NS-fed and HS-fed rats, focusing on the active-to-inactive transition, we identified NR3C1 and PRL as the key upstream regulators affected by diet. The GR signaling and the circadian clock are linked, with GR influencing the expression of clock genes and the clock controlling GR activity (39, 40). PRL has been shown to exhibit a circadian rhythm in its excretion in humans (41). Also, in mice lacking CLOCK, PRL-induced signaling was significantly decreased (42). PRL and GR are known to regulate specific signaling pathways synergistically, such as the JAK/STAT pathway in lactation (reviewed in Ref. 43). However, no studies have been reported on the kidney. The interactions between PRL and NR3C1 were suggested to be related to the body's "response to lipid" in the STRING analysis. Both PRL and NR3C1 can affect the expression of PDK4 (44, 45), which we also observed in our data as a downstream target. Nevertheless, it is essential to note that upstream regulators are predictions, and the transcripts themselves do not necessarily need to change.

One of the more interesting findings in our study was a predicted shift in energy source from lipids to glucose in response to time-of-day and dietary salt. More ATP-demanding tissues, such as proximal tubules in the kidney, tend to prefer fatty acids as their source of energy rather than glucose (reviewed in Ref. 46). Given that our data are derived from cortical tissue, which contains a larger proportion of proximal tubules, the shift toward fatty acid oxidation during the active period under baseline conditions makes physiological sense. In certain disease conditions, including cancer, diabetes, and cardiovascular disease, a well-documented phenomenon known as the Warburg effect is observed, characterized by an energy shift from fatty acid (mitochondrial) oxidative phosphorylation to aerobic glycolysis (reviewed in Refs. 47–50). This process is an adaptation by the disease cells to function under the malignant conditions often found in tumors or other tissues undergoing injury. A metabolic shift such as this has been reported previously in Dahl SS rats' cardiac tissue during ventricular hypertrophy and heart failure (51, 52). Furthermore, disruptions in circadian rhythm have also been reported to trigger such metabolic adaptations (53). Nevertheless, to the best of our knowledge, a Warburg-like effect has not been reported in relation to time-of-day in salt-loading stress in the kidney or in the context of SS HTN before.

The "gatekeeper" of changing the substrate use of energy between lipids and carbohydrates is the PDC (*Pdha1*), which regulates the entry of glycolytic products into the TCA cycle (reviewed in Ref. 32). Its activity is regulated by PDKs and PDPs, which inactivate or reactivate it via phosphorylation and dephosphorylation. In nocturnal SS rats on an NS diet, *Pdk4* mRNA expression increased at night, promoting fatty

Figure 7. Summary of the transcriptomic analysis of genotypic effect ($SS^{Per1-/-}$ vs. SS) in the inactive period of the rat. Network of upstream regulators and downstream DEGs for normal-salt-fed (*A*) and high-salt-fed (*B*) $SS^{Per1-/-}$ vs. SS—analyses in the inactive period. *C*: top 20 canonical pathways enhanced in male $SS^{Per1-/-}$ vs. SS during inactive period. IPA-predicted upstream molecules that may be causing the observed gene expression changes. A few upstream regulators, based on their activation *z*-scores and relationships to one another, are chosen to create these networks. A $-\log(P \text{ value}) > 1.3$ was considered significant for canonical pathways. $n = 5$ or 6 rats per group. IPA uses the *P* value of overlap, calculated using the right-tailed Fisher's exact test, to identify significant pathways. The overall activation/inhibition states of canonical pathways are predicted based on a *z*-score algorithm. The coloring of the pathways was based on the activation status provided by IPA. IPA, Ingenuity Pathway Analysis; SS, salt sensitive.

acid oxidation. An HS diet, however, caused a regulatory shift. Concurrently, the phosphorylation level of PDH is significantly higher during the active period than during the inactive period, indicating PDC inactivation. This contradicts the findings from transcriptomics and indicates a decoupling at the level of PTMs. One possible explanation is that the HS diet functions as a physiological stressor, disrupting the anticipatory, slow-acting transcriptional clock mechanism and forcing the cell to rely on rapid, nongenomic, and ion-sensitive protein kinase cascades to maintain acute metabolic control. This reactive PTM is likely to involve constitutive PDK isoforms (PDK2) or severe inhibition of PDPs, overriding the failure of the suppressed circadian transcriptional input. However, our data showed an increase in *Pdp2* expression with HS, though the activity of the proteins and expression of these genes may differ.

Another theoretical possibility of a rapid nongenomic signaling pathway in SS rats that causes a decoupling of transcriptional and PTM levels is aldosterone, which has been predicted to affect rapid modifications of various kinases independent of transcriptional levels (54). Aldosterone, together with AGT and IL1B, was also suggested to be the major upstream regulators of the transcriptome of the $SS^{Per1-/-}$ model fed a HS diet in the inactive period. Interestingly, in the $SS^{Per1-/-}$ model compared with SS, we observed a higher plasma aldosterone level in our previous study conducted during the inactive period (8). In the current study, when fed an HS diet, $SS^{Per1-/-}$ rats exhibited a lower level of phosphorylation compared with SS rats in the S293 region of PD, coupled with increased transcript level of *Pdk4*. This indicates that if there is such a rapid response in SS rats challenged with a HS diet that decouples the transcript and PTM, it is not present in the $SS^{Per1-/-}$ rats.

The insights from phosphoproteomics also highlighted the possibility of PTMs in NDRG1, which is phosphorylated by SGK1, whose transcripts were significantly increased in both NS-fed SS rats during the active compared with inactive period and HS-fed $SS^{Per1-/-}$ rats compared with SS in the inactive. A recent study also reported that SGK1 plays a role in the day/night difference and the morning surge in blood pressure (55). NDRG1 is a protein that helps cells adapt to low-oxygen conditions (56), which may be relevant to the metabolic shift observed under HS stress.

We reported that *Per1* absence (in HS-fed $SS^{Per1-/-}$ vs. SS during the inactive period) is associated with predicted disruptions in metabolic, immune, and circadian adaptations. Interpreting pathway analyses in omics is challenging because unbiased pathways can yield predictions unrelated to tissues or diseases of interest, such as "sperm mortality" in our kidney transcriptomics. To overcome this challenge, given that many pathways share second messengers or common signal mechanisms, we examined the top pathways and used existing knowledge to understand the practical implications of the pathway predictions. By taking a closer look at the DEGs involved in pathway activation in $SS^{Per1-/-}$ versus SS rats on an HS diet during inactivity, several pathway groups could be identified. For instance, cardiac hypertrophy signaling, Myc-mediated apoptosis signaling, and endothelin-1 signaling use cAMP signaling. Such close examination of the top 20 pathways suggests a signaling cascade involving glutathione metabolism and cytokines that modulate β-adrenergic signaling, which, in turn, affects cAMP signaling and ultimately regulates circadian rhythms. Therefore, future studies using the $SS^{Per1-/-}$ model integrating this signaling cascade could be meaningful.

Despite the significant findings of this study, several limitations should be acknowledged. Although all other conditions were controlled, the RNA-Seq analysis of the NS-fed groups and HS-fed groups was performed separately and not directly compared. Proteomics and PTM analyses were performed only in the HS-fed groups. All our analyses are based solely on data from male animals. Related to the study of circadian rhythms defined in the strictest sense, it should be noted that our studies were performed on animals in a typical 12:12 light:dark cycle. Our two time-point collections do not allow us to draw any direct conclusions regarding a phase shift. Future studies should be performed under constant conditions, such as total darkness, to ascertain circadian effects from diurnal effects. Our data are also limited to the renal cortex and may omit insights from the medullary fraction. Furthermore, since all current conclusions are drawn from omics analyses, they need further functional studies to be translated into clinical relevance. However, these findings could enhance our understanding of blood pressure regulation and dietary stress, especially in cases of circadian rhythm disruption, such as those experienced by shift workers.

Conclusions

In summary, we generated a comprehensive dataset that enables detailed exploration of the interactions among dietary salt intake, time-of-day, and the genetic ablation of *Per1*. In Dahl SS rats, we predicted substantial metabolic adaptations in the renal cortex, reflected in time-of-day-dependent transcriptomic changes, particularly under dietary salt stress. These alterations suggest a switch between lipid- and glucose-based energy utilization that occurs independently of synchronized blood pressure rhythms. Furthermore, the lack of *Per1* was predicted to be contributing to the effects observed with dietary salt increase, which could explain the exacerbated SS HTN and the desynchrony of the blood pressure rhythm in $SS^{Per1-/-}$ rats.

DATA AVAILABILITY

The data that support the findings of this study are available in MATERIALS AND METHODS, RESULTS, and/or SUPPLEMENTAL MATERIAL of this article. RNA-Seq data are publicly available through Gene Expression Omnibus (GEO) under accession GSE311806.

SUPPLEMENTAL MATERIAL

Supplemental Tables S1–S8: https://doi.org/10.6084/m9.figshare.31378747.

Supplemental Figs. S1–S5: https://doi.org/10.6084/m9.figshare.31378699.

ACKNOWLEDGMENTS

The authors gratefully acknowledge Elizabeth Wood, Director of the Morsani College of Medicine Proteomics Core at the University of South Florida, for the assistance with proteomic

analysis and related methods. The authors also thank the developers of the open-source software STRING, Phospho-Analyst, R, InteractiVenn, and Phosphomatics.

GRANTS

Research in the author's laboratory was supported by the National Institutes of Health grants R01 DK135644 and R01 DK129227 (to A.S.), R01 DK109570 (to M.L.G. and A.S.), and T32 HL160529 (to R.B.); U.S. Department of Veteran Affairs grants I01 BX004024 and IK6 RD001204 (to A.S.); American Heart Association 25POST1375066 (to L.V.D.) and 25POST1374965 (to A.Z.); and USF Hypertension and Kidney Research Center Early Stage Investigator grants (to L.V.D., A.Z., R.T., and O.K.) and Multi-PI grant (to A.S.). Proteomic analysis was supported in part by the Morsani College of Medicine Proteomics core at the University of South Florida.

DISCLAIMERS

The contents do not represent the views of the Department of Veterans Affairs or the United States Government.

DISCLOSURES

No conflicts of interest, financial or otherwise, are declared by the authors.

AUTHOR CONTRIBUTIONS

L.V.D.: Conceptualization, Data curation, Formal analysis, Investigation, Writing – original draft, Writing – review & editing; A.Z.: Conceptualization, Data curation, Formal analysis, Investigation, Writing – review & editing; R.T.: Formal analysis, Methodology, Writing – review & editing; M.L.: Data curation, Investigation, Writing – review & editing; O.K.: Data curation, Formal analysis, Writing – review & editing; V.L.: Data curation, Investigation, Writing – review & editing; R.B.: Investigation, Writing – review & editing; M.L.G.: Conceptualization, Writing – review & editing; A.S.: Conceptualization, Funding acquisition, Project administration, Resources, Writing – review & editing.

REFERENCES

1. **Bailey MA**, **Dhaun N.** Salt sensitivity: causes, consequences, and recent advances. *Hypertension* 81: 476–489, 2024. doi:10.1161/HYPERTENSIONAHA.123.17959.
2. **Faulkner JL**, **Belin de Chantemèle EJ.** Female sex, a major risk factor for salt-sensitive hypertension. *Curr Hypertens Rep* 22: 99, 2020. doi:10.1007/s11906-020-01113-6.
3. **Demirci M**, **Afolabi JM**, **Kirabo A.** Aging and sex differences in salt sensitivity of blood pressure. *Clin Sci (Lond)* 139: 199–212, 2025. doi:10.1042/CS20240788.
4. **Kimura G**, **Dohi Y**, **Fukuda M.** Salt sensitivity and circadian rhythm of blood pressure: the keys to connect CKD with cardiovascular events. *Hypertens Res* 33: 515–520, 2010. doi:10.1038/hr.2010.47.
5. **Firsov D**, **Bonny O.** Circadian rhythms and the kidney. *Nat Rev Nephrol* 14: 626–635, 2018. doi:10.1038/s41581-018-0048-9.
6. **Costello HM**, **Johnston JG**, **Juffre A**, **Crislip GR**, **Gumz ML.** Circadian clocks of the kidney: function, mechanism, and regulation. *Physiol Rev* 102: 1669–1701, 2022. doi:10.1152/physrev.00045.2021.
7. **Soliman RH**, **Pollock DM.** Circadian control of sodium and blood pressure regulation. *Am J Hypertens* 34: 1130–1142, 2021. doi:10.1093/ajh/hpab100.
8. **Zietara A**, **Spires DR**, **Juffre A**, **Costello HM**, **Crislip GR**, **Douma LG**, **Levchenko V**, **Dissanayake LV**, **Klemens CA**, **Nikolaienko O**, **Geurts AM**, **Gumz ML**, **Staruschenko A.** Knockout of the circadian clock protein PER1 (Period1) exacerbates hypertension and increases kidney injury in dahl salt-sensitive rats. *Hypertension* 79: 2519–2529, 2022. doi:10.1161/hypertensionaha.122.19316.
9. **Kita Y**, **Shiozawa M**, **Jin W**, **Majewski RR**, **Besharse JC**, **Greene AS**, **Jacob HJ.** Implications of circadian gene expression in kidney, liver and the effects of fasting on pharmacogenomic studies. *Pharmacogenetics* 12: 55–65, 2002. doi:10.1097/00008571-200201000-00008.
10. **Costello HM**, **Juffre A**, **Cheng KY**, **Bratanatawira P**, **Crislip GR**, **Zietara A**, **Spires DR**, **Staruschenko A**, **Douma LG**, **Gumz ML.** The circadian clock protein PER1 is important in maintaining endothelin axis regulation in Dahl salt-sensitive rats. *Can J Physiol Pharmacol* 101: 136–146, 2023. doi:10.1139/cjpp-2022-0134.
11. **Costello HM**, **Grenier C**, **Ivy JR**, **Czopek A**, **Jones NK**, **Krilis G**, **Stewart K**, **Nespoux J**, **Holmes MC**, **Livingstone DEW**, **Dhaun N**, **Bailey MA.** Chronic ACTH infusion alters the diurnal rhythm of sodium excretion, inducing nondipping blood pressure and salt-sensitivity in male mice. *Hypertension* 82: 1754–1766, 2025. doi:10.1161/hypertensionaha.124.24473.
12. **Mohri T**, **Emoto N**, **Nonaka H**, **Fukuya H**, **Yagita K**, **Okamura H**, **Yokoyama M.** Alterations of circadian expressions of clock genes in dahl salt-sensitive rats fed a high-salt diet. *Hypertension* 42: 189–194, 2003. doi:10.1161/01.HYP.0000082766.63952.49.
13. **Fujii T**, **Uzu T**, **Nishimura M**, **Takeji M**, **Kuroda S**, **Nakamura S**, **Inenaga T**, **Kimura G.** Circadian rhythm of natriuresis is disturbed in nondipper type of essential hypertension. *Am J Kidney Dis* 33: 29–35, 1999. doi:10.1016/S0272-6386(99)70254-4.
14. **Bankir L**, **Bochud M**, **Maillard M**, **Bovet P**, **Gabriel A**, **Burnier M.** Nighttime blood pressure and nocturnal dipping are associated with daytime urinary sodium excretion in African subjects. *Hypertension* 51: 891–898, 2008. doi:10.1161/hypertensionaha.107.105510.
15. **Fukuda M**, **Munemura M**, **Usami T**, **Nakao N**, **Takeuchi O**, **Kamiya Y**, **Yoshida A**, **Kimura G.** Nocturnal blood pressure is elevated with natriuresis and proteinuria as renal function deteriorates in nephropathy. *Kidney Int* 65: 621–625, 2004. doi:10.1111/j.1523-1755.2004.00419.x.
16. **Gumz ML**, **Stow LR**, **Lynch IJ**, **Greenlee MM**, **Rudin A**, **Cain BD**, **Weaver DR**, **Wingo CS.** The circadian clock protein Period 1 regulates expression of the renal epithelial sodium channel in mice. *J Clin Invest* 119: 2423–2434, 2009. doi:10.1172/jci36908.
17. **Curtis AM**, **Cheng Y**, **Kapoor S**, **Reilly D**, **Price TS**, **FitzGerald GA.** Circadian variation of blood pressure and the vascular response to asynchronous stress. *Proc Natl Acad Sci USA* 104: 3450–3455, 2007. doi:10.1073/pnas.0611680104.
18. **Yang G**, **Chen L**, **Zhang J**, **Ren B**, **FitzGerald GA.** Bmal1 deletion in mice facilitates adaptation to disrupted light/dark conditions. *JCI Insight* 5: e125133, 2019. doi:10.1172/jci.insight.125133.
19. **Pati P**, **Fulton DJR**, **Bagi Z**, **Chen F**, **Wang Y**, **Kitchens J**, **Cassis LA**, **Stepp DW**, **Rudic RD.** Low-salt diet and circadian dysfunction synergize to induce angiotensin II-dependent hypertension in mice. *Hypertension* 67: 661–668, 2016. doi:10.1161/hypertensionaha.115.06194.
20. **Zhang D**, **Jin C**, **Obi IE**, **Rhoads MK**, **Soliman RH**, **Sedaka RS**, **Allan JM**, **Tao B**, **Speed JS**, **Pollock JS**, **Pollock DM.** Loss of circadian gene Bmal1 in the collecting duct lowers blood pressure in male, but not female, mice. *Am J Physiol Renal Physiol* 318: F710–F719, 2020. doi:10.1152/ajprenal.00364.2019.
21. **Yunker L**, **Usa K**, **Williams AC**, **Reho JJ**, **Grobe JL**, **Gumz ML**, **Kriegel AJ.** Time-restricted feeding attenuates salt-sensitive hypertension and renal damage. *Hypertension* 82: 1743–1753, 2025. doi:10.1161/hypertensionaha.125.24857.
22. **Wiśniewski JR**, **Zougman A**, **Nagaraj N**, **Mann M.** Universal sample preparation method for proteome analysis. *Nat Methods* 6: 359–362, 2009. doi:10.1038/nmeth.1322.
23. **Cox J**, **Hein MY**, **Luber CA**, **Paron I**, **Nagaraj N**, **Mann M.** Accurate proteome-wide label-free quantification by delayed normalization and maximal peptide ratio extraction, termed MaxLFQ. *Mol Cell Proteomics* 13: 2513–2526, 2014. doi:10.1074/mcp.M113.031591.
24. **Tyanova S**, **Temu T**, **Sinitcyn P**, **Carlson A**, **Hein MY**, **Geiger T**, **Mann M**, **Cox J.** The Perseus computational platform for comprehensive analysis of (prote)omics data. *Nat Methods* 13: 731–740, 2016. doi:10.1038/nmeth.3901.
25. **Krämer A**, **Green J**, **Pollard J Jr**, **Tugendreich S.** Causal analysis approaches in ingenuity pathway analysis. *Bioinformatics* 30: 523–530, 2014. doi:10.1093/bioinformatics/btt703.

26. **Szklarczyk D**, **Kirsch R**, **Koutrouli M**, **Nastou K**, **Mehryary F**, **Hachilif R**, **Gable AL**, **Fang T**, **Doncheva NT**, **Pyysalo S**, **Bork P**, **Jensen LJ**, **von Mering C.** The STRING database in 2023: protein-protein association networks and functional enrichment analyses for any sequenced genome of interest. *Nucleic Acids Res* 51: D638–D646, 2023. doi:10.1093/nar/gkac1000.
27. **Francavilla C**, **Lupia M**, **Tsafou K**, **Villa A**, **Kowalczyk K**, **Rakownikow Jersie-Christensen R**, **Bertalot G**, **Confalonieri S**, **Brunak S**, **Jensen LJ**, **Cavallaro U**, **Olsen JV.** Phosphoproteomics of primary cells reveals druggable kinase signatures in ovarian cancer. *Cell Rep* 18: 3242–3256, 2017. doi:10.1016/j.celrep.2017.03.015.
28. **Heberle H**, **Meirelles GV**, **da Silva FR**, **Telles GP**, **Minghim R.** InteractiVenn: a web-based tool for the analysis of sets through Venn diagrams. *BMC Bioinformatics* 16: 169, 2015. doi:10.1186/s12859-015-0611-3.
29. **Yang H**, **Xia L**, **Chen J**, **Zhang S**, **Martin V**, **Li Q**, **Lin S**, **Chen J**, **Calmette J**, **Lu M**, **Fu L**, **Yang J**, **Pan Z**, **Yu K**, **He J**, **Morand E**, **Schlecht-Louf G**, **Krzysiek R**, **Zitvogel L**, **Kang B**, **Zhang Z**, **Leader A**, **Zhou P**, **Lanfumey L**, **Shi M**, **Kroemer G**, **Ma Y.** Stress–glucocorticoid–TSC22D3 axis compromises therapy-induced antitumor immunity. *Nat Med* 25: 1428–1441, 2019. doi:10.1038/s41591-019-0566-4.
30. **Sierra-Ramos C**, **Velazquez-Garcia S**, **Keskus AG**, **Vastola-Mascolo A**, **Rodríguez-Rodríguez AE**, **Luis-Lima S**, **Hernández G**, **Navarro-González JF**, **Porrini E**, **Konu O**, **Alvarez de la Rosa D.** Increased SGK1 activity potentiates mineralocorticoid/NaCl-induced kidney injury. *Am J Physiol Renal Physiol* 320: F628–F643, 2021. doi:10.1152/ajprenal.00505.2020.
31. **Kadmiel M**, **Cidlowski JA.** Glucocorticoid receptor signaling in health and disease. *Trends Pharmacol Sci* 34: 518–530, 2013. doi:10.1016/j.tips.2013.07.003.
32. **Park S**, **Jeon JH**, **Min BK**, **Ha CM**, **Thoudam T**, **Park BY**, **Lee IK.** Role of the pyruvate dehydrogenase complex in metabolic remodeling: differential pyruvate dehydrogenase complex functions in metabolism. *Diabetes Metab J* 42: 270–281, 2018. doi:10.4093/dmj.2018.0101.
33. **Leeming MG**, **O'Callaghan S**, **Licata L**, **Iannuccelli M**, **Lo Surdo P**, **Micarelli E**, **Ang CS**, **Nie S**, **Varshney S**, **Ameen S**, **Cheng HC**, **Williamson NA.** Phosphomatics: interactive interrogation of substrate-kinase networks in global phosphoproteomics datasets. *Bioinformatics* 37: 1635–1636, 2021. doi:10.1093/bioinformatics/btaa916.
34. **Li X.** SIRT1 and energy metabolism. *Acta Biochim Biophys Sin (Shanghai)* 45: 51–60, 2013. doi:10.1093/abbs/gms108.
35. **Abdul-Wahed A**, **Guilmeau S**, **Postic C.** Sweet Sixteenth for ChREBP: established roles and future goals. *Cell Metab* 26: 324–341, 2017. doi:10.1016/j.cmet.2017.07.004.
36. **Nishimoto M**, **Griffin KA**, **Wynne BM**, **Fujita T.** Salt-sensitive hypertension and the kidney. *Hypertension* 81: 1206–1217, 2024. doi:10.1161/HYPERTENSIONAHA.123.21369.
37. **Tiwari R**, **Kravtsova O**, **Dissanayake LV**, **Lowe M**, **Xu B**, **Levchenko V**, **Didik S**, **Bohovyk R**, **Ilatovskaya DV**, **Palygin O**, **Staruschenko A.** Longitudinal multi-organ transcriptomic atlas of salt-induced hypertension (Preprint). *bioRxiv* 2025. doi:10.1101/2025.08.27.672714.
38. **Yamaguchi S**, **Mitsui S**, **Yan L**, **Yagita K**, **Miyake S**, **Okamura H.** Role of DBP in the circadian oscillatory mechanism. *Mol Cell Biol* 20: 4773–4781, 2000. doi:10.1128/MCB.20.13.4773-4781.2000.
39. **Ivy JR**, **Jones NK**, **Costello HM**, **Mansley MK**, **Peltz TS**, **Flatman PW**, **Bailey MA.** Glucocorticoid receptor activation stimulates the sodium-chloride cotransporter and influences the diurnal rhythm of its phosphorylation. *Am J Physiol Renal Physiol* 317: F1536–F1548, 2019. doi:10.1152/ajprenal.00372.2019.
40. **Ivy JR**, **Oosthuyzen W**, **Peltz TS**, **Howarth AR**, **Hunter RW**, **Dhaun N**, **Al-Dujaili EAS**, **Webb DJ**, **Dear JW**, **Flatman PW**, **Bailey MA.** Glucocorticoids induce nondipping blood pressure by activating the thiazide-sensitive cotransporter. *Hypertension* 67: 1029–1037, 2016 [Erratum in *Hypertension* 68: e5, 2016]. doi:10.1161/hypertensionaha.115.06977.
41. **Waldstreicher J**, **Duffy JF**, **Brown EN**, **Rogacz S**, **Allan JS**, **Czeisler CA.** Gender differences in the temporal organization of proclactin (PRL) secretion: evidence for a sleep-independent circadian rhythm of circulating PRL levels- a clinical research center study. *J Clin Endocrinol Metab* 81: 1483–1487, 1996. doi:10.1210/jcem.81.4.8636355.
42. **Yuzhen C**, **Zheng F.** The effect of circadian rhythm on prolactin/PRLR-mediated intracellular signaling profiles in vivo and in vitro. *Tissue Cell* 73: 101570, 2021. doi:10.1016/j.tice.2021.101570.
43. **Hu X**, **Li J**, **Fu M**, **Zhao X**, **Wang W.** The JAK/STAT signaling pathway: from bench to clinic. *Signal Transduct Target Ther* 6: 402, 2021. doi:10.1038/s41392-021-00791-1.
44. **Connaughton S**, **Chowdhury F**, **Attia RR**, **Song S**, **Zhang Y**, **Elam MB**, **Cook GA**, **Park EA.** Regulation of pyruvate dehydrogenase kinase isoform 4 (PDK4) gene expression by glucocorticoids and insulin. *Mol Cell Endocrinol* 315: 159–167, 2010. doi:10.1016/j.mce.2009.08.011.
45. **Arumugam R**, **Horowitz E**, **Noland RC**, **Lu D**, **Fleenor D**, **Freemark M.** Regulation of islet beta-cell pyruvate metabolism: interactions of prolactin, glucose, and dexamethasone. *Endocrinology* 151: 3074–3083, 2010. doi:10.1210/en.2010-0049.
46. **Mitrofanova A**, **Merscher S**, **Fornoni A.** Kidney lipid dysmetabolism and lipid droplet accumulation in chronic kidney disease. *Nat Rev Nephrol* 19: 629–645, 2023. doi:10.1038/s41581-023-00741-w.
47. **Chen Z**, **Liu M**, **Li L**, **Chen L.** Involvement of the Warburg effect in non-tumor diseases processes. *J Cell Physiol* 233: 2839–2849, 2018. doi:10.1002/jcp.25998.
48. **Kuspriyanti NP**, **Ariyanto EF**, **Syamsunarno MRAA.** Role of Warburg effect in cardiovascular diseases: a potential treatment option. *TOCMJ* 15: 6–17, 2021. doi:10.2174/1874192402115010006.
49. **Liberti MV**, **Locasale JW.** The warburg effect: how does it benefit cancer cells? *Trends Biochem Sci* 41: 211–218, 2016 [Erratum in *Trends Biochem Sci* 41: 287, 2016]. doi:10.1016/j.tibs.2015.12.001.
50. **Shimada S**, **Hoffmann BR**, **Yang C**, **Kurth T**, **Greene AS**, **Liang M**, **Dash RK**, **Cowley AW.** Metabolic responses of normal rat kidneys to a high salt intake. *Function (Oxf)* 4: zqad031, 2023. doi:10.1093/function/zqad031.
51. **Kato T**, **Niizuma S**, **Inuzuka Y**, **Kawashima T**, **Okuda J**, **Tamaki Y**, **Iwanaga Y**, **Narazaki M**, **Matsuda T**, **Soga T**, **Kita T**, **Kimura T**, **Shioi T.** Analysis of metabolic remodeling in compensated left ventricular hypertrophy and heart failure. *Circ Heart Fail* 3: 420–430, 2010. doi:10.1161/CIRCHEARTFAILURE.109.888479.
52. **Fillmore N**, **Levasseur JL**, **Fukushima A**, **Wagg CS**, **Wang W**, **Dyck JRB**, **Lopaschuk GD.** Uncoupling of glycolysis from glucose oxidation accompanies the development of heart failure with preserved ejection fraction. *Mol Med* 24: 3, 2018. doi:10.1186/s10020-018-0005-x.
53. **Blask DE**, **Dauchy RT**, **Dauchy EM**, **Mao L**, **Hill SM**, **Greene MW**, **Belancio VP**, **Sauer LA**, **Davidson L.** Light exposure at night disrupts host/cancer circadian regulatory dynamics: impact on the Warburg effect, lipid signaling and tumor growth prevention. *PLoS One* 9: e102776, 2014. doi:10.1371/journal.pone.0102776.
54. **Cheng L**, **Poulsen SB**, **Wu Q**, **Esteva-Font C**, **Olesen ETB**, **Peng L**, **Olde B**, **Leeb-Lundberg LMF**, **Pisitkun T**, **Rieg T**, **Dimke H**, **Fenton RA.** Rapid aldosterone-mediated signaling in the DCT increases activity of the thiazide-sensitive NaCl cotransporter. *J Am Soc Nephrol* 30: 1454–1470, 2019. doi:10.1681/asn.2018101025.
55. **Al-Qusairi L**, **Basquin D**, **Roy A**, **Stifanelli M**, **Rajaram RD**, **Debonneville A**, **Nita I**, **Maillard M**, **Loffing J**, **Subramanya AR**, **Staub O.** Renal tubular SGK1 deficiency causes impaired K^+ excretion via loss of regulation of NEDD4-2/WNK1 and ENaC. *Am J Physiol Renal Physiol* 311: F330–F342, 2016. doi:10.1152/ajprenal.00002.2016.
56. **Cangul H.** Hypoxia upregulates the expression of the NDRG1 gene leading to its overexpression in various human cancers. *BMC Genet* 5: 27, 2004. doi:10.1186/1471-2156-5-27.